IEEE Access
Multidisciplinary ⋮ Rapid Review ⋮ Open Access Journal

Received April 1, 2022, accepted April 26, 2022, date of publication May 2, 2022, date of current version May 12, 2022.

Digital Object Identifier 10.1109/ACCESS.2022.3171850

Biometric Information Recognition Using Artificial Intelligence Algorithms: A Performance Comparison

SUNUSI BALA ABDULLAHI[1,2], (Member, IEEE), CHAINARONG KHUNPANUK[3], ZAKARIYYA ABDULLAHI BATURE[4], HARUNA CHIROMA[5], NUTTAPOL PAKKARANANG[3], AUWAL BALA ABUBAKAR[6,7], AND ABDULKARIM HASSAN IBRAHIM[8]

[1]Department of Computer Engineering, Faculty of Engineering, King Mongkut's University of Technology Thonburi, Bangkok 10140, Thailand
[2]Zonal Criminal Investigation Department, Nigeria Police, Louis Edet House Force Headquarters, Abuja 900221, Nigeria
[3]Mathematics and Computing Science Program, Faculty of Sciences and Technology, Phetchabun Rajabhat University, Phetchabun 67000, Thailand
[4]Department of Electronics and Telecommunication Engineering, Faculty of Engineering, King Mongkut's University of Technology Thonburi, Bangkok 10140, Thailand
[5]Future Technology Research Center, National Yunlin University of Science and Technology, Douliu 64002, Taiwan
[6]Numerical Optimization Research Group, Department of Mathematical Sciences, Faculty of Physical Sciences, Bayero University Kano, Kano 700006, Nigeria
[7]Department of Mathematics and Applied Mathematics, Sefako Makgatho Health Sciences University, Ga-Rankuwa, Pretoria 0204, South Africa
[8]KMUTT Fixed Point Research Laboratory, Room SCL 802 Fixed Point Laboratory, Science Laboratory Building, Department of Mathematics, Faculty of Science, King Mongkut's University of Technology Thonburi (KMUTT), Bangkok 10140, Thailand

Corresponding author: Chainarong Khunpanuk (iprove2000ck@gmail.com)

ABSTRACT Addressing crime detection, cyber security and multi-modal gaze estimation in biometric information recognition is challenging. Thus, trained artificial intelligence (AI) algorithms such as Support vector machine (SVM) and adaptive neuro-fuzzy inference system (ANFIS) have been proposed to recognize distinct and discriminant features of biometric information (intrinsic hand features and demographic cues) with good classification accuracy. Unfortunately, due to nonlinearity in distinct and discriminant features of biometric information, accuracy of SVM and ANFIS is reduced. As a result, optimized AI algorithms ((ANFIS) with subtractive clustering (ANFIS-SC) and SVM with error correction output code (SVM-ECOC)) have shown to be effective for biometric information recognition. In this paper, we compare the performance of the ANFIS-SC and SVM-ECOC algorithms in their effectiveness at learning essential characteristics of intrinsic hand features and demographic cues based on Pearson correlation coefficient (PCC) feature selection. Furthermore, the accuracy of these algorithms are presented, and their recognition performances are evaluated by root mean squared error (RMSE), mean absolute percentage error (MAPE), scatter index (SI), mean absolute deviation (MAD), coefficient of determination (R^2), Akaike's Information Criterion (AICc) and Nash-Sutcliffe model efficiency index (NSE). Evaluation results show that both SVM-ECOC and ANFIS-SC algorithms are suitable for accurately recognizing soft biometric information on basis of intrinsic hand measurements and demographic cues. Moreover, comparison results demonstrated that ANFIS-SC algorithms can provide better recognition accuracy, with RMSE, AICc, MAPE, R^2 and NSE values of ≤ 3.85, 2.39E+02, 0.18%, ≥ 0.99 and ≥ 99, respectively.

INDEX TERMS ANFIS, artificial intelligence, biometric features recognition, demographic cues, SVM, misclassifications, optimization.

I. INTRODUCTION

The geometric models for biometric hand features (skin fingerprint and palm model) are easy to hack in contrast with biometric bones-based system (phalangeal biometric models). This is because hand geometric model is based on external measurement of hand features (hand patterns; knuckle creases) which are highly exposable. Suspects leave traces everyday and everywhere they have utilized biometric resources. Even more aggravating, if suspects have committed crimes, third party presence or interfering on the same system might have defeated biometric cue traces when

The associate editor coordinating the review of this manuscript and approving it for publication was Anandakumar Haldorai.

matching sample to suspect. However, in cyberspace context, utilization of external hand measurements and/or knuckle creases may allow criminals to easily utilize information of legitimate users for unauthorized access or activities. Another limitation of these features is that, it does not favor victims of skin diseases, in a situation where top layers of their skin (palm and fingerprints) are affected [1]. Thus, victims may no longer get access to any external hand measurement-based biometric recognition system, even if they have fully recovered [1], [2]. However, these problems might have defeated crime detection, accident rescue, amnesia victims identification, missing persons, unknown deceased, and cyberspace authentication. In contrast, the phalangeal biometric model require intrinsic hand features such as length/width of Proximal Phalanx, Distal Phalanx etc. which are not as exposed as their counterparts [2]. Therefore, hand biometric recognition based on intrinsic measurement of human bones stand as solution for human identification and crime detection. Moreover, an appropriate selection of intrinsic hand features yield an excellent result [3]. Due to these reasons, evaluation of intrinsic hand features based on demographic cues by learning models aid in recognizing biometric hand information. It is well known that recognition of biometric hand features and demographic cues is a complex non-linear procedure that happens by a complex interaction of different redundant hand features. Pearson Correlation coefficient (PCC) features selection is generally appreciated as a stable feature representation of complex and non-linear dynamical behaviour of hand biometric information. This analysis minimize models training complexity, and reduce misclassification during recognition. Recognition from selective intrinsic hand features by PCC is an effective and reliable method for critical infrastructure.

Studies of human demographic characteristics from biometric hand features have been extensively proved in the body of literature purposely on Artificial Intelligence (AI) learning or descriptive statistics analysis. It is being documented that external hand features (geometric features) are deployed in biometric recognition, such information involves measurement of lengths, circumference, thickness, width of fingers, palm, wrist, skin texture etc. to predict human sex, age, and human height [4]. Karki and Singh demonstrate a strong relationship between the pattern of fingerprints and human gender [5]. Meanwhile, in [6] relationship of biometric information in cross-domain identity recognition is demonstrated. Among well-known biometric gesture recognition method is Discriminant analysis [7], which was followed by descriptive statistics approaches [8]. Likewise, Thakar *et al.* propose method of gender determination using ridge characteristics and ridge density of fingerprints. These features were statistically analyzed and their results proved the usefulness of biometric information in determining demographic information [9]. Another variation of the descriptive statistics model is a bootstrap estimate, where a large number of sample sizes similar to actual samples are drawn with replacement from samples, and desired statistic was determined within each sample. Bootstrap fails to approximate different ratios if they belong to similar finger measurements [10]. Linear and curvilinear regression models were built to investigate two hundred and fifty (250) students using measurements of their height, hand length and breadth to predict gender. However, these models return low accuracy, features are not robust for biometric predictions [11]. In [12] Stevenage *et al.* proposed method to demonstrate restrictions while matching a suspect hand, analysis was carried out using Analysis of Variance (ANOVA).

As visited from the literature above, these models may not provide good prediction results, which lead to wrong conclusions. Misclassification from descriptive statistics, such as linear or curvilinear is correlated to cut-off point and there is no cut-off value that should be optimal. Nevertheless, AI algorithms are independent of any value of this cut-off. In addition, misclassifications from classical and analytical statistics approaches happen because of nonlinearity from biometric features and model parameter settings. To handle nonlinearity of biometric features, AI algorithms remain as good choice [13], [14]. Multiple AI algorithms are combined using a fuzzy inference system, where hand geometry is particularly considered as intrinsic biometric cues from near-infrared human hand images to locate interphalangeal joints of human fingers [2]. The paper employed pulse response, hand geometry and finger vein using Convolutional Neural Network fuzzy (CNN-fuzzy) inference for detection of a live human body to improve performance against counterfeit attempts [2]. A part from the fuzzy recognition algorithms, Alias and Radzi [15], adopted an SVM for fingerprint classification. Gavrilova *et al.* in [16], used kinect sensor to extract human emotion cues in multimodal context, which are trained with SVM classifier. Recognition of human hand gestures is performed using ECOC-SVM [17]. Their results indicate feasibility of using SVM in real-world applications. Henceforth, to further explore the capabilities of AI-based algorithms to learn intrinsic hand features in human demographic cues recognition, SVM demonstrates to be better as it strikes a better balance between nonlinear feature points to predict four demographic information (sex, height, foot size, and log-weight) [18]. The results obtained using the above-mentioned AI algorithms are quite promising and motivated us to explore other AI-based algorithms for recognition of demographic cues from biometric information. However, the major drawback of all these algorithms is that they do not prove to be robust in case of nonlinear features and have large parameter computation which lead to low accuracy. Therefore, to further explore the capabilities of AI-based algorithms and to overcome the drawbacks of different parameters estimation, the Error Correction Output Code (ECOC) scheme is used with Pearson correlation coefficient features (PCC) to recognize the demographic cues from biometric hand features.

Inspired by the above contributions, in this paper, we compare the performance of two improved AI algorithms for high-precision recognition of demographic cues from

biometric hand features. The first algorithm is composed of SVM and Error correction output code (ECOC), namely SVM-ECOC with PCC. ECOC algorithm is robust in handling unreliable and noisy features. It has benefit to minimize a single multi-class problem [19]–[21]. The second algorithm is composed of Adaptive Neuro-fuzzy Inference System (ANFIS) optimized by subtractive clustering (SC) with least square approximation, namely ANFIS-SC with PCC. SC has good estimating capability to ANFIS parameters, and it is robust in high dimensional data for moderate features. These two algorithms are validated using distinct intrinsic hand features selected using PCC from biometric and physiological hand data set in [18]. In what follows, we give an outline of the contributions made in this paper.

(a) We investigate the impact of intrinsic hand features on biometric information recognition.
(b) We extend PCC technique for selecting key hand biometric features to ease AI recognition/learning algorithm.
(c) Some of the available optimization schemes are employed to avoid redundant parameter estimation of AI learning algorithms, so that the dimensions of parameter vector are reduced and the computational accuracy is improved.
(d) Computational comparison is carried out between ANFIS-SC and SVM-ECOC algorithm to illustrate the high efficiency of the ANFIS-SC algorithm.
(e) Increase in recognition accuracy is the major contribution of this article in the field of biometric crime detection and human identification.
(f) Numerical results show that the ANFIS-SC algorithm maximizes recognition performance for soft biometric cues.

Organization of our paper proceeds as follows: related state-of-the-art methods, research gap, motivation, and contributions formed Section I. The details of ANFIS, and SVM are described in Section II. This section also dealt with the optimization procedures of our adopted algorithms. Section III described data description and its characteristics. It also dealt with PCC test, feature extractions and selections, recognition phase, parameter settings, and performance metrics. Section IV give out results of the AI recognition algorithms and their various performance evaluations. It also interpreted performance comparison between our works and some existing model, and running time. Conclusion, applications and limitations as well as future direction formed Section V. To make more precise explanation, we list the notations used throughout the article in Table 1.

TABLE 1. Nomenclature.

Notations	Descriptions
ANFIS	adaptive neuro-fuzzy inference system
A and B	membership functions for inputs h
h_i	set of input features
η_i , ω_i , Ω_i	consequent parameters
f	fused output
χ	node output
l_d and ϵ_d	parameters of Sigmoid membership function
$\overline{T_d}$	normalized firing strength
l	layer order
d	node order combination
$u_c(h_i)$	respective joint set
$\lambda_c(h_i)$	multi-valued set
ϵ_i and l_i	premise parameters
O_i	observed output dataset
O'_i	recognized output dataset
S	number of samples
θ	number of parameters
σ_r^2	standard deviation
O_a	mean observed data
ϑ_i	density index
b_c	thickness
b_l	positive constant value
$\aleph$	maximum number of iterations
h_l	left hand features
h_r	right hand features
WB	wrist breadth
WL	wrist to little
WR	wrist to ring
WM	wrist to middle
WI	wrist to index
WT	wrist to thumb
LPP	little proximal phalanx
LIP	little intermediate phalanx
LDP	little distal phalanx
RPP	ring proximal phalanx
RIP	ring intermediate phalanx
RDP	ring distal phalanx
MPP	middle proximal phalanx
MIP	middle intermediate phalanx
MDP	middle distal phalanx
IPP	index proximal phalanx
IIP	index intermediate phalanx
IDP	index distal phalanx
TPP	thumb proximal phalanx
TDP	thumb distal phalanx
HB	hand breadth
O_i^s	set of outputs for sex
O_i^h	set of output for height
O_i^b	set of output for weight
O_i^f	set of output for foot-size
b	bias
w	normal vector in SVM hyperplane
$\frac{b}{\|\mathbf{w}\|_2}$	parameter determines the offset of the hyperplane
$\frac{2}{\|w\|}$	distance between two hyperplanes
λ	represent parameter which increase margin
ξ_i	smallest nonnegative number
c	box constraint
$\phi(h_i)$	hand features in transformed shape
γ	parameter for kernel adjusting
COV	covariance
φ	give relationship of two independent parameters
Fit	model fitness
X	minimum Hamming distance among pair of code words
LOG	logistic regression
H	hand gesture space
υ	dichotomizer
F	random coding matrix
κ	codewords
T(.)	Time complexity

II. MATERIALS AND METHODS

Artificial intelligence (AI) is superior technique when there is a nonlinearity problem among biometric features recognition. AI can handle problems that have non-linear solutions irrespective of fitness of non-linear features. In addition, AI learning approach is suitable when needed to solve biometric features within certain time. Exploiting the benefits of AI algorithm, we proposed to build features from PCC [22] into optimized AI algorithm. PCC-based feature selection

minimized features dimensionality [23] and AI learning complexity. This section describe architectures of the following adopted AI algorithms; (a) ANFIS-SC (b) SVM-ECOC and steps of the methods are described in flowchart 1.

A. ADAPTIVE NEURO-FUZZY INFERENCE SYSTEM (ANFIS)

ANFIS is an AI approach, composing Artificial Neural Network (ANN) and fuzzy inference networks (FIS) as a single ANFIS model, leveraging individual limitations of ANN and FIS methods [24], [25]. One major advantage of ANFIS is its ability to make good representation of complex and non-linear connections among features [24]. In addition, its soft computing and rapid convergence raised interest of using ANFIS in prediction of complicated relationships [26]–[29]. ANFIS aim to enhance/optimize FIS parameters by referring learning protocol according to input-output relationship vector. ANFIS optimization is carried out such that calibration errors among trained samples and original samples are minimized [13]. The following equations define and describe ANFIS:

Here two inputs combination are used to formulate ANFIS layers, for two inputs there exists linear and nonlinear parameters, where A and B rule from 1*st* and 2*nd* order Sugeno FIS utilized η_1, η_2, Ω_1, Ω_2, ω_1 and ω_2 as consequent parameters, so that τ of h_i tunes in ϵ_1; τ of h_i tunes in Ω_1; and τ of h_i, tunes in ϵ_2, and τ of h_2 tunes in Ω_2, respectively. The output of the system is illustrated by $\chi_{\iota,d}$. Where ι and d stand for order and node order combination respectively. Henceforth, 1*st* and 2*nd* fuzzy rules could be produced from the combination of two hand input feature sets h_i as:

$$A = \eta_1 h_i + \omega_1 h_i + \Omega_1;$$
$$B = \eta_2 h_i + \omega_2 h_i + \Omega_2.$$

where η_i, ω_i, and Ω_i denote consequent parameters. According to two fuzzy rules, feed-forward layers of ANFIS can be designed as follows:

Layer One: The nodes are adaptive here and fulfills quantifier rule, then node output can be given as:

$$\chi_{1,d} = \tau_{\epsilon,1}(h_i), \quad d = 1, 2, \tag{1}$$

where l_d and ϵ_d denote premise parameters, that determine shape of Gaussian membership function (MF). The Gaussian MF is given in Eq. (2),

$$\tau_{\epsilon_1}(h_i) = \frac{1}{1 + e^{-\epsilon_d(h_i - l_d)}}. \tag{2}$$

Layer Two: Contain fixed nodes. It calculates explosion power per each rule, which is given as:

$$\chi_{2,d} = T_d = \tau_{\epsilon_1}(h_i) \times \epsilon_{\Omega_1}(t), \quad d = 1, 2. \tag{3}$$

Layer Three: The nodes are fixed in this layer. The output of this layer is called normalized firing strength $\overline{T_d}$, formulated as:

$$\chi_{3,d} = \overline{T_d} = \frac{T_d}{\sum_1^2 T_d}, \quad d = 1, 2. \tag{4}$$

Layer Four: This layer consist of adaptive nodes. It calculate consequent parameters from successive node as product of $\overline{T_d}$ and the first order polynomial. It output is given as:

$$\chi_{4,d} = \overline{T_d}\, f_d = \overline{T_d}\,(\eta_d h_d + \omega_d h_d + \Omega_d). \tag{5}$$

Layer five: This layer has single fixed node Σ. It computes the input signals from all antecedent layers. Function of this layer $Z_{5,i}$ could be calculated using:

$$\chi_{5,d} = \sum_d \overline{T_d} f_d = \frac{\sum_d T_d\, f_d}{\sum_d T_d}. \tag{6}$$

However, from Eq. (6), $\overline{f_d}$ can be estimated to be nearly equal to the original information with respect to the observed function f_d, so that demographic cues could be recognized for any available intrinsic hand features. But one main challenge is how to produce recognized demographic cues to be nearly equal to the original intrinsic hand gestures, therefore, this brought matter of minimizing function, which is defined as follows:

$$\chi_{5,d} = min \sum_{d=1}^{t} [\overline{f_d}(h_d, \cdots, h_{d,t}) - f_d\ ]^2. \tag{7}$$

However, ANFIS layers Eqs. (1)-(7) suffer from thorny-parameter estimation, which seriously lead to noise during recognition. Nature-inspired optimizers [30]–[32] played significant role in estimating ANFIS parameters. In contrast, parameter estimation is achieved through clustering mechanisms. Clustering serve as robust technique to handle cluster information. Therefore, empowering ANFIS with clustering is a substitute to nonlinear features estimation. There exist other ANFIS parameter estimations according to clustering mechanism such as: Fuzzy C-mean (FCM); which optimize ANFIS parameters by minimizing FCM-based derived objective function. Its major limitation is inability to estimate large number of parameters [25], [33]. Grid partition algorithm (GP); effectively handle ANFIS parameters for small sample size, its flexibility is due to inherent large amount of rules and parameters generation. However, its main challenge is inherent exponential growth of fuzzy rules due to increase in sample size [25]. Subtractive clustering (SC); where generated clusters are utilized to derive iterative-based optimization clustering to estimate ANFIS parameters. This method has good representation, if high dimensional case is utilized for moderate biometric hand features [25], [32]. Optimization of ANFIS parameters using SC achieved best performance [34].

1) SUBTRACTIVE CLUSTERING (SC)

In SC, every biometric features are considered as competent cluster centre. The competent cluster over entire input-output feature pose is computed as their Euclidean distance equation over the whole feature poses. The poses having high competent greater than the threshold value are considered cluster centers. The primary concept is to calculate the density index ϑ_i, corresponding to the biometric hand features

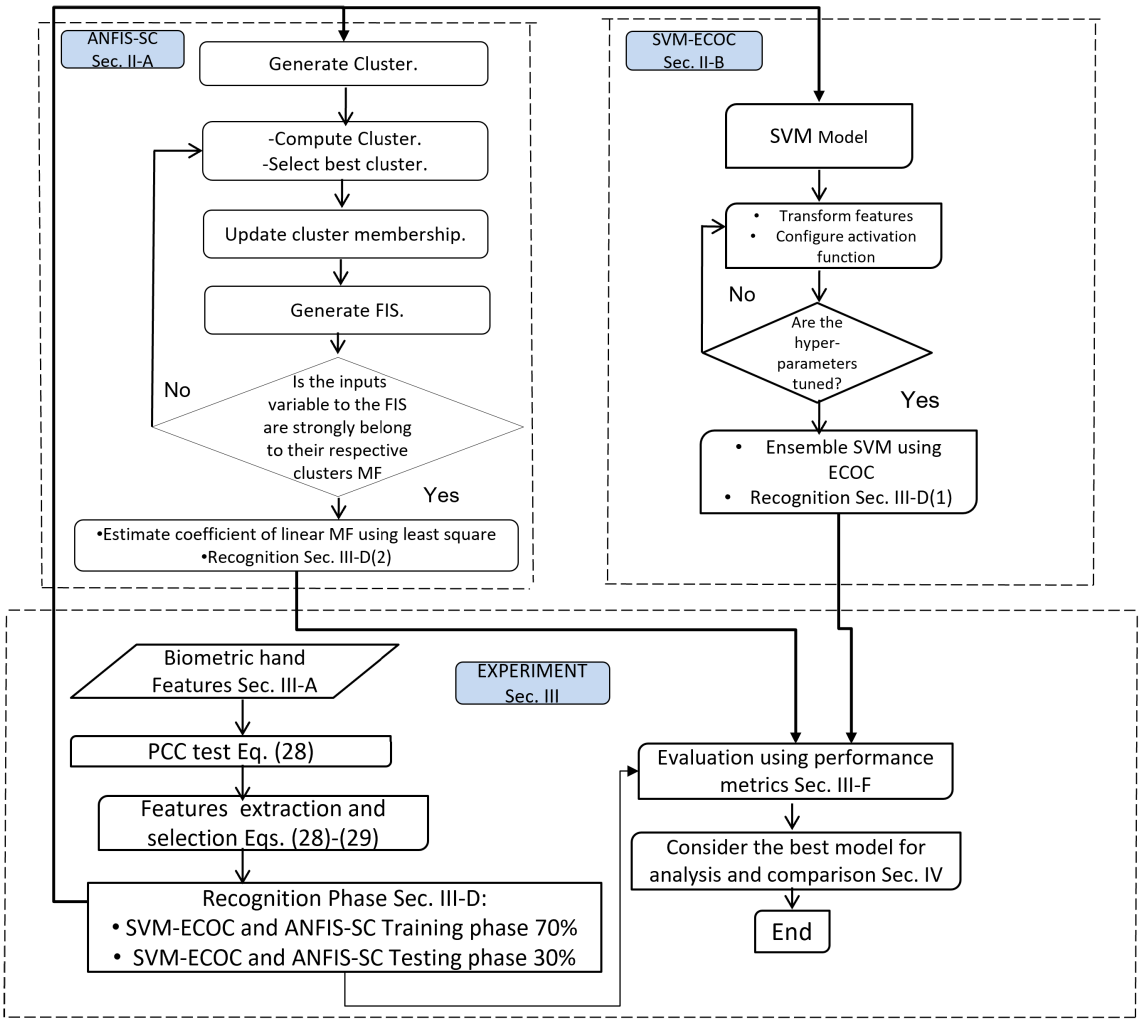

FIGURE 1. Proposed method flowchart.

h_i having positive constant b_t (determine distance between cluster centres), which is given as:

$$\vartheta_i = \sum_{i=1}^{S} exp(-\frac{||h_i - h_k||^2}{(\frac{b_n}{2})^2}). \tag{8}$$

Henceforth, SC algorithm decides to select topmost density index as the first cluster center which is modified as:

$$\vartheta_1 = \vartheta_i - \vartheta_{h1} exp(-\frac{||h_i - h_{h1}||^2}{(\frac{a_o}{2})^2}). \tag{9}$$

We have chosen feature with high competent as next cluster centre. This loop in Eq. (9) is iterated until the stopping criteria is achieved. The cluster centres are utilized to generate fuzzy rules and parameters which lead to design FIS model. The rules are fuzzified using Eq. (2), which adaptively alter characteristics of FIS to make the pattern looks like corresponding antecedent function. The major contribution to the existing ANFIS-SC is made on lines 9-17 in Algorithm 1, where we fine tune FIS and ANFIS-based model every iterations with presently labeled recognizer (calculated cluster).

Therefore, computed clusters are applied to generate iterative optimization-based clustering for ANFIS model parameters identification [34]. In this paper, number of cluster centers are set to be 14 for 112 biometric hand pose $h_1, h_2, \cdots, h_D$. Every biometric hand pose represents a particular member of cluster centre. Thus, making same amount of fuzzy rules set Ω and cluster centres, and each correspond to features of cluster. Formulation Eq. (9) is iterated until convergence, which lead to achieve sufficient cluster centres. Biometric hand features vector is fuzzified by adopting Gaussian MF with sigmoid activation (hybrid MFs), which yield membership degree per each feature (equals to $112 \times \Omega$). As a result, raises dimensionality of the biometric hand features input vector. The hybrid MFs allow smooth transition among linear and nonlinear parameters, when compared to triangular and trapezoidal MFs [35]. In addition, hybrid MF has less parameters in contrast with bell and triangular MF thus make it more flexible. Therefore, Gaussian MFs is formulated as in Eq. (2). However, *ith* rule can be obtained as follows: if $in_1 = \tau_1^i$, and $in_2 = \tau_2^i, \cdots, in_{112} = \tau_{112}^i$,

hence output is given as f_i. Where $i = 1 : \tau$. Then, first order Sugeno-type fuzzy model for τ_n^i at *ith* MF and *jth* hand intrinsic features dimension, where $n = 1 : 112$, is moderated as:

$$f_i = \eta_1^i in_1 + \eta_2^i in_2 + \cdots + \eta_{112}^i in_{112} + \omega_i, \tag{10}$$

where $[\eta_1^i, \cdots, \eta_{112}^i, \omega_i]$ denote consequent parameters. The premise parameters are obtained from τ_n^i Gaussian MF Eq. (2). Tuning the values of these parameters will vary MF, and also alter behaviors of FIS. FIS union is described as follows:

$$\tau_n^i(in_n) = \frac{1}{1 + e^{-\epsilon_i(in_n - l_{in})}}, \tag{11}$$

where l_{in} denotes *nth* element of cluster centre l_i and ϵ_i denotes radius of neighborhood. However, we estimated consequent parameters using least-squares estimation method. Finally, output of Sugeno-type fuzzy algorithm is computed with Eq. (6). Then, defining $\eta_i = [\eta_1^i, \eta_2^i, \cdots, \eta_{112}^i]$ as row vector of linear parameters $\eta_1^i \cdots, \eta_{112}^i$ and $H = [in_1, in_2, \cdots, in_{112}]^T$ denote hand intrinsic gestures space, then substituting for f_i in Eq. (6), it becomes:

$$\chi = \sum_{i=1}^{\Omega} \overline{T_i}(\eta_i H + \omega_i). \tag{12}$$

B. SUPPORT VECTOR MACHINE (SVM)

SVM is an artificial intelligence classifier, applies to nonlinear data recognition and classification. SVM gain superiority among classical machine learning and AI classifiers in daily life application due to flexibility and ease-of-use for handling various classification issues [36]. One benefit of SVM is the modeling and conversion of a dimension for high altitude pattern recognition problems, empirical risk minimization, efficient learning, and good generalization ability [37]. The SVM model formulation is defined by letting h_i to be the extracted features from both left and right hand, h_l and h_r respectively. Then we let O_i^s, O_i^q, O_i^p, O_i^f to represent set of outputs for sex, height, weight, and foot-size respectively where $i = 1 : n$ samples of measured data. In short biometric hand information used for training comprises of sample and label pairs as: $D_t = (h_i, O_i^s) : i = 1, 2, 3, \ldots, 112$. Where $h_i \in O_i^s$, each class O_i^s represent male or female (1 or -1). Therefore, hyper-plane can be used to separate cluster h_i which belongs to either $O_i^s = 1$ and $O_i^s = -1$. Hyper-plane can be formulated using set of hand poses h_i satisfying the following equation;

$$f(h) = w^T \cdot h_i + b = 0, \tag{13}$$

where w is a vector of n row features and b denote bias which is constant. Therefore w and b can be solved using finest separating plane. Now w can be formulated as;

$$\mathbf{w} = \sum_{i=1}^{n} \alpha_i O_i^s h_i. \tag{14}$$

Algorithm 1 ANFIS-SC

start
set $a_o, b_o, h_i^s, h_i^q, h_i^p, h_i^f, E$ {inputs}
Output $O_i^s, O_i^q, O_i^p, O_i^f$
set τ_n {FIS}
set MF {membership function}
set $Iter.$ {max. iteration no.}
initialize SC
generate MF using h_i
compute φ_i in Eq. (8)
modify Eq. (8) to get φ_1 in Eq. (9)
update φ_i
generate FIS using STEP 11
repeat
  if $h_i \in \varphi_i$ **do**
  update FIS in Eq. (12)
  evaluate $\Theta(FIS, M)$ Eq. (12)
  do estimate ANFIS parameters
  else
  repeat STEPS 10-13
  else if
  estimate STEP 16
  else
  repeat from STEP 8
until Eq. (7) converge
return Eq. (12)
stop
Get O_i' best model using Eqs. (29) and (32)
compute AI parameters Eqs. (30), (33), (34), and (40).
end

To solve for b there is need to minimize $||w||$ such that biometric hand features vector can be given as (h_i, O_i^s)

$$\mathbf{b} = \frac{1}{n} \sum_{i=1}^{n} (O_i^s - w \cdot h_i), \tag{15}$$

where c_i is a box constraint. Hence, distance between hyper-planes is $\frac{2}{||w||}$. Thus, to maximize distance, there is need to minimize $||w||$. To avoid any hand pose to fall within hyper-plane margin, there is need to add constraints so that each hand pose must fall on its correct margin side as follows;
$w^T h_i - b \geq 1$, if $O_i^s = 1$ and
$w^T h_i - b \leq 1$, if $O_i^s = -1$. Which can be rewritten as;

$$O_i^s(w^T h_i - b \geq 1), \quad for\ all\ 1 \leq i \leq n, \tag{16}$$

$min.||W||$ subject to $O_i^s(w^T h_i - b \geq 1)$, for $i = 1, \ldots, n$. However, support vectors can be realized from maximum hyper-plane margin which is completely determine by closet h_i to margin. Support vectors are h_i on boundary, those for which

$$O_i^s f(h_i) = 1. \tag{17}$$

Therefore, Eq. (17) can not fit to non-linear biometric features. Thus, Hinge loss function is very useful for hand poses

that are linearly non-separable $max(0, 1 - O_i^s(w^T h_i - b))$, where O_i^s and $w^T h_i - b$ denote desired output (1 or -1), and actual output respectively. Now Eq. (16) is configured with Hinge loss function and becomes Eq. (18).

$$\frac{1}{n}[\sum_{i=1}^{n} max(0, 1 - O_i^s(w^T h_i - b))] + \lambda||w||^2, \tag{18}$$

where λ represent parameter which increase margin for h_i to fall within rightful side and $\lambda||w||^2$ represent loss function. For simplifying Eq. (18), we let $\xi_i = max(0, 1-O_i^s(w^T h_i-b))$ for every $i \in \{1, 2, \ldots, n\}$ as minimum non-negative number, which satisfy $\xi_i = max(0, 1-O_i^s(w^T h_i-b) \geq 1-\xi)$. Therefore, optimization problem in Eq. (18) becomes Eq. (19) at some conditions:

$$\frac{1}{n}\sum_{i=1}^{n} \xi_i + \lambda||w||^2. \tag{19}$$

Under conditions of $\xi_i = O_i^s(w^T h_i - b) \geq 1 - \xi$ and $\xi \geq 0$, for every i. To swap among maximizing distance between 1 and -1 from Eq. (19) we now added a box constraint parameter c, where $c = 0.05$. Furthermore, to achieve maximum non-linear separation among classes, it is imperative to transform biometric features h_i. This can allow to achieve high dimension projection. However, available SVM kernel function such as Polynomial, Radial Basis Function (RBF), Hyperbolic tangent are highly robust for high dimension projection and efficiency of SVM model. Although, RBF kernel function achieved best performance [38]. RBF is known as Gaussian kernel which is mostly applied to non-linear data such as biometric hand poses. Since SVM general equations are formulated, then we are now to handle classification on our proposed hand intrinsic features on it transformed shape $\phi(h_i)$ and configuring RBF kernel function. RBF can be given as follows:

$$R(h_i, h_j) = \phi(h_i) \cdot \phi(h_j). \tag{20}$$

We now configure RBF kernel function in Eq. (20), then it becomes:

$$R(h_1, h_2) = \exp(-\gamma||h_i - \tilde{h_i}). \tag{21}$$

where $\tilde{h_i}$ represent hand intrinsic features, γ represent parameter for kernel adjusting. For $\gamma > 0$ and sometimes represented as $\gamma = 1/(2\sigma^2)$. The values of γ and c are hyper-parameters tuned to attain optimum SVM model with RBF kernel. Then, value of γ defines influence and extent to which training hand poses attain. Lower value means 'far' while higher value means 'close', higher value of γ result in good accuracy. However, c find model tolerance towards misclassification, its low value yield low accuracy for SVM model while its high value yield good accuracy but may result to failure in generalization. We settled these hyper-parameters with middle values. Finally, we can achieved SVM classifier with $w = \sum_{i=1}^{n} c_i O_i^s \phi(h_i)$, c_i which can be obtained through Error Correcting Output Code (ECOC) optimization problem solution. Classifier is equivalently given as:

$$\begin{aligned} f(c_1 \ldots c_n) &= \sum_{i=1}^{n} c_i - \frac{1}{2}\sum_{i=1}^{n}\sum_{j=1}^{n}(O_i^s c_i(\phi(h_i)\phi(h_j)O_j^s c_j) \\ &= \sum_{i=1}^{n} c_i - \frac{1}{2}\sum_{i=1}^{n}\sum_{j=1}^{n}(O_i^s c_i R(h_i, h_j)O_j^s c_j) \end{aligned} \tag{22}$$

Eq. (22) can be achieved by the following conditions:
$\sum_{i=1}^{n} c_i O_i^s h_i$ and $0 \leq c_i \leq \frac{1}{2n\lambda}$ for every i. However, optimized b can be obtained from the following:

$$b = w^T \cdot \phi(h_i) - O_i^s = [\sum_{j=1}^{n} O_i^s c_i \phi(h_j) \cdot \phi(h_i)] - O_i^s \tag{23}$$

It is worthy noting, that SVM algorithm is designed for a binary classification, which need ensemble ECOC strategy for multi-classification problem [17]. ECOC is adopted to handle samples with unreliable or noisy information [39]. Application of ECOC is extended to multi-classification SVM algorithm to minimize single multi-class problem. Theoretical background of ECOC is provided in the following section II-C. The concept behind SVM multi-class classification problem of non-linear mapping with soft computing is achieved from modified SVM using ensemble ECOC design.

C. ERROR CORRECTING OUTPUT CODE (ECOC)

The ideology of ECOC, implies, the coding/decoding over the scheme itself. Its input consists of set E classes, with e set of binary partition classes, that are considered as potential dichotomizers, which are learned against the partitions. Therefore, codeword having length e is achieved per class, inside codeword each bit matches output of dichotomizer: usually coded by $+1$ or -1 based on their classes and set of membership. Aligning the codeword in a matrix shape, such that matrix F, it is defined as $F \in [-1, +1]^{E \times e}$. In this case, the matrix F is coded with five dichotomizers [19] $[\upsilon_1, \cdots, \upsilon_5]$ with respect to four class problem $[s_1, \cdots, s_4]$ and codewords $[\kappa_1, \cdots, \kappa_4]$. The goal of the alignment is to learn the input sets with respect to label $[(h_1, D_1), \cdots, (h_n, D_n)]$ at a given input sets and labels D_l. Considering Fig. 2, entries with orange and red represents $+1$ and -1 for dichotomizer and null inside matrix F. Thus, learning of first classifier is to distinguish among s_3 versus s_1, s_2 and s_4, whereas the learning behavior of second classifier is to recognize s_2 and s_3 versus s_1 and s_4. Moreover, ECOC is also encoded on ternary schemes as shown in Fig. 2b. In ternary symbol-based ECOC, symbol zero is added, which lead to the generation of seven dichotomizers $[\upsilon_1, \cdots, \upsilon_7]$ per matrix, thus the coding matrix and codewords for a four class problem is obtained as $F \in [-1, 0, +1]^{E \times e}$ and $[\kappa_1, \cdots, \kappa_4]$, respectively. Therefore, the computation of dichotomizers can be formulated as follows:

$$\upsilon_1(z) = \begin{cases} +1, & if \quad z \in [s_3]. \\ -1, & if \quad z \in [s_1, s_2, s_4], \cdots, \end{cases} \tag{24}$$

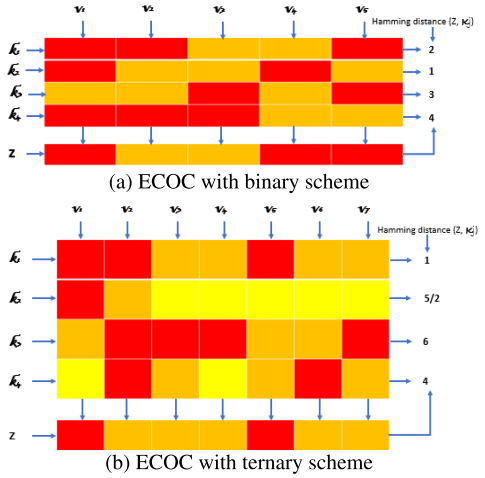

FIGURE 2. ECOC code from four class argument.

$$\upsilon_5(z) = \begin{cases} +1, & if \quad z \in [s_2, s_4]. \\ -1, & if \quad z \in [s_1, s_3]. \end{cases} \tag{25}$$

The principle of decoding is shown in Fig. 2. The code z is realized when employing binary classifiers e, per each input sets h_i during verification. Therefore, z is collated with root code words ($\kappa_i, i \in [1, \cdots E]$) of each class, which is defined in F. These input sets are allocated to the closest code word from available schemes such as Hamming decoding, inverse Hamming decoding, and euclidean decoding. The second decoding strategy in ECOC is referred as ternary decoding. Ternary decoding is performed from any of attenuated euclidean decoding, loss-based decoding, and probabilistic-based decoding [40]–[42]. For ternary scheme, Hamming decoding strategy classify the validation input sets by class s_1. However, the validation codeword do not include the zero bit, this is because the response per dichotomizer is given as $\upsilon_j \in [-1, +1]$. For details of this scheme authors are encouraged to read [19]–[21]. Inspired by the above benefits, in this paper, we extended application of ternary ECOC on SVM binary learners. The major contribution to the existing SVM-ECOC is made on lines 12-28 in Algorithm 1, where we fine tune the SVM-ECOC model every 10 iterations with presently labeled recognizer. We achieved finest combination of SVM-ECOC with suitable RBF kernel and box constraint.The rest of the parameter combinations are reported in Table 10.

Algorithm 2 SVM-ECOC

1: **start**
2: **set** $w, b, h_i^s, h_i^q, h_i^p, h_i^f, E$ {inputs}
3: **Output** $O_i^s, O_i^q, O_i^p, O_i^f$
4: **set** $\gamma, c_i, iteration.$
5: **initialize** *SVM* Eq. (13)
6: **min.** w in Eq. (14) to solve for b in (15)
7: **if** Eq. (16) is satisfied
8: **do** max. hyper-plane margin
9: **else**
10: **configure** $\lambda||w||^2$ in Eq. (18)
11: **end if**
12: **transform** h_i in Eq. (20)
13: **configure** γ in Eq. (21) and choose c_i in Eq. (22)
14: **update** Eq. (18) using STEPS 14-16
15: **repeat**
16: **construct** F matrix
17: **if** $F \in [-1, +1]^{E \times e}$ **do**
18: **compute** dichotomizers in Eq. (24)
19: **else**
20: **generate** $F \in [-1, 0, +1]^{E \times e}$
21: **end if**
22: **if** length h_i is $2^{E-1} - 1$ **do**
23: **choose** ternary scheme
24: **min** $\frac{E(E-1)}{2}$ and $\psi < \frac{E(E-1)}{2}$
25: **display** CORRECT CLASS
26: **else**
27: **repeat** STEPS 16-24
28: **until** Eq. (23) converge
29: **end if**
30: **return** Eq. (13)
31: **stop**
32: **Get** b best model using Eqs. (29) and (32)
33: **compute** AI parameters Eqs. (30), (33), (34), and (38).
34: **end**

III. EXPERIMENT

The reviewed literature highlighted the understanding of the principal practices to achieve best performance and efficiency. Based on the reviewed literature, the biometric and physiological data set was taken for experimental investigation and a flowchart was designed to achieve the paper objective.

A. BIOMETRIC HAND FEATURES

We adopted biometric and physiological data set in [18]. The data was extracted from 112 participants (with equal number of male and female to be 56). The participants were all Caucasians aged within 18 to 35 years. Demographic information gathered from the participants consisted of sex (male or female), height, weight and foot size. Demographic descriptive analysis is extended from the work in [18]. The steps for the proposed methods are explained in flow chart Fig. 1. The extracted biometric hand features model are defined by letting h_i to be the extracted features from both left and right hand, h_l and h_r respectively, such that each h_i contained; Wrist Breadth *WB*, Wrist to Little*WL*, Wrist to Ring *WR*, Wrist to Middle *WM*, Wrist to Index *WI*, Wrist to Thumb *WT*, Little Proximal Phalanx *LPP*, Little Intermediate Phalanx *LIP*, Little Distal Phalanx *LDP*, Ring Proximal Phalanx *RPP*, Ring Intermediate Phalanx *RIP*, Ring Distal Phalanx *RDP*, Middle Proximal Phalanx *MPP*, Middle Intermediate Phalanx *MIP*, Middle Distal Phalanx *MDP*, Index Proximal Phalanx *IPP*, Index Intermediate Phalanx *IIP*, Index Distal Phalanx *IDP*, Thumb Proximal Phalanx *TPP*, Thumb Distal Phalanx *TDP*,

Hand breadth *HB*. Then we let $O_i^s, O_i^q, O_i^p, O_i^f$ to represent set of outputs for sex, height, weight, and foot-size respectively, where $i = 1 : n$ samples of measured data. In short biometric information used for training comprises of sample and label pairs as: $D_t = (h_i, O_i^s) : i = 1, 2, 3, \ldots, 112$. Where $h_i \in O_i^s$, each class O_i^s represent male or female (1 or -1).

B. PEARSON CORRELATION COEFFICIENT (PCC)

We first consider Pearson's correlation coefficient (PCC) to investigate most significant and reliable features for algorithms training. PCC test is successful to give insight and clues in choosing best model features in real applications [43], [44]. Another reason for PCC test is to minimize AI learning complexity. Here, φ denotes two parameters that are independent between (h_i, O_i), the covariance among those variables is donated by COV, having their respective standard deviations as σ_{h_i} and σ_{O_i}. Therefore, PCC is explained by:

$$\varphi = \frac{COV(h_i, O_i)}{\sqrt{\sigma_{h_i}.\sigma_{O_i}}} \tag{26}$$

Results of test are displayed on Tables 2 - 9. The Tables demonstrated that eleven (11) hand intrinsic features are independent of each other, with the exception that some samples have independent correlation between features less than 0.5, which is statistically negligible. Each table demonstrate PCC between features. Diagonal entries stand for the correlation of a particular feature with itself. Any cell that has value not less than 0.5 is assume to possess high correlation. We can deduced that majority of features are highly correlated. There are some few features with lower correlation and may be preserved. These correlational patterns were found to be steady among data of participants. Nevertheless, these features can still be chosen as independent variables. The significant features will be selected, and procedures for that will be explained in the next section.

C. FEATURE EXTRACTIONS AND SELECTIONS

Now features have been defined and evaluated using Eq. (26). For better understanding of evaluated features, we measured importance and significance of these features using coefficient of determination R metrics, as shown in Figs. 3 - 4. Feature correlation was explored because of its possibility in feature reduction. It is pointed that more compact feature set will lessen complexity of AI learning and exclude dropping important variances. Features relationship is illustrated in Tables 2-5. Since biometric features vector β_i contain hand features h_i, then the feature selection M can be treated as maximization problem, which is formulated using

$$M = \max_{\beta \in [0,1]^i} \left\{ \frac{\sum_{l=1,u=1}^{i} (h_i \beta_i)^2}{\sum_{l=1}^{i} (\beta_i) + \sum_{u \neq l}^{i} 2 \times (h_l \beta_l \beta_{l,u})} \right\} \tag{27}$$

We averaged significant features and emphasize on feature fusion $\tilde{\beta}$ which decrease training complexity of the AI model. The performance of fused features 5, with regards to the rate

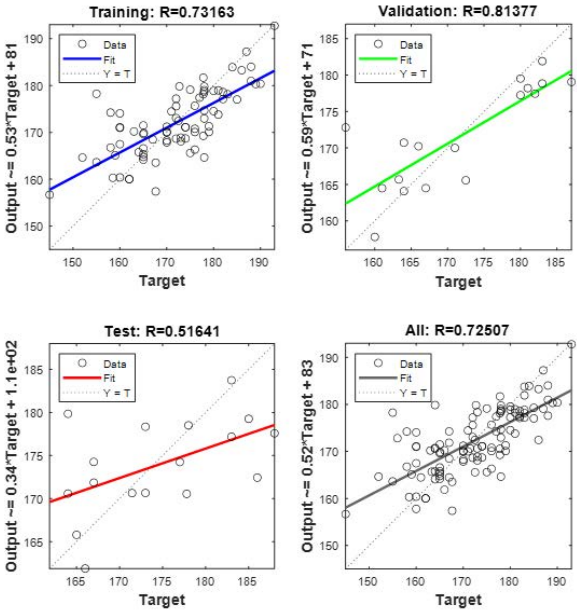

FIGURE 3. Correlational analysis of selected features.

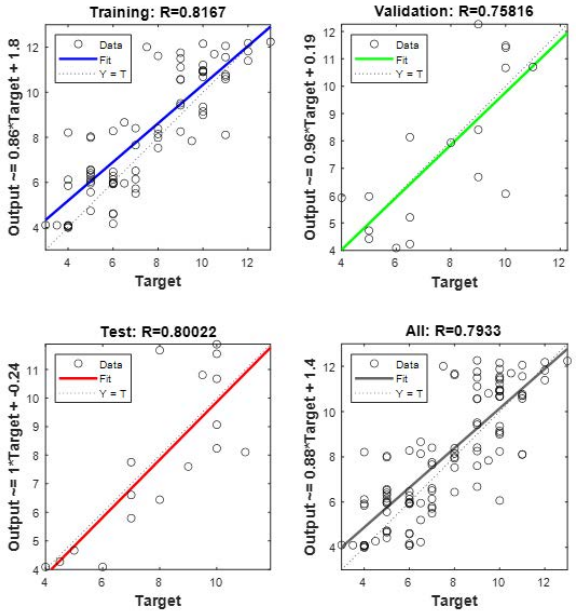

FIGURE 4. Correlational analysis of selected features.

of recognition, would be discussed in brief. In this experiment, we design our input features vector from the following selected input information:

(a) Seven (7) features for height recognition from right hand are selected as shown in Table 2.
(b) Nine (9) features for height recognition from left hand as shown in Table 3.
(c) Three (3) features for sex recognition from right hand as shown in Table 4.
(d) Two (2) features for sex recognition from left hand as shown in Table 5.

TABLE 2. Statistical confidence of selected features for Height from right-hand.

Features	WI	RDP	MPP	MIP	IIP	IDP	TPP	HEIGHT
WI	1							
RDP	0.6261	1						
MPP	0.49947	0.45375	1					
MIP	0.67735	0.61333	0.38286	1				
IIP	0.52421	0.53539	0.3648	0.6732	1			
IDP	0.5621	0.55029	0.49481	0.35377	0.22157	1		
TPP	0.54903	0.51896	0.48349	0.45384	0.40624	0.46422	1	
HEIGHT	0.68936	0.67771	0.2618	0.56851	0.54269	0.44685	0.36172	1

TABLE 3. Statistical confidence of selected features for Height from left-hand.

Features	WL	WR	WI	LPP	RPP	RDP	MPP	IPP	IDP	HEIGHT
WL	1									
WR	0.95026	1								
WI	0.7664	0.81675	1							
LPP	0.3114	0.34553	0.41133	1						
RPP	0.40286	0.34726	0.53369	0.65768	1					
RDP	0.57131	0.25747	0.63978	0.33981	0.5312	1				
MPP	0.46891	0.45421	0.50513	0.61532	0.75986	0.75874	1			
IPP	0.55134	0.42006	0.38052	0.49563	0.49724	0.51043	0.5188	1		
IDP	0.475	0.43185	0.34887	0.37332	0.42665	0.49613	0.53344	0.51454	1	
HEIGHT	0.62243	0.53565	0.68831	0.33473	0.48588	0.51867	0.54242	0.42088	0.53353	1

TABLE 4. Statistical confidence of selected features for Sex from right-hand.

Features	WB	WL	LPP	SEX
WB	1			
WL	0.54148	1		
LPP	0.35268	0.28324	1	
SEX	0.75521	0.64521	0.26944	1

TABLE 5. Statistical confidence of selected features for Sex from left-hand.

Features	WB	WT	SEX
WB	1		
WT	0.63839	1	
SEX	0.69385	0.69428	1

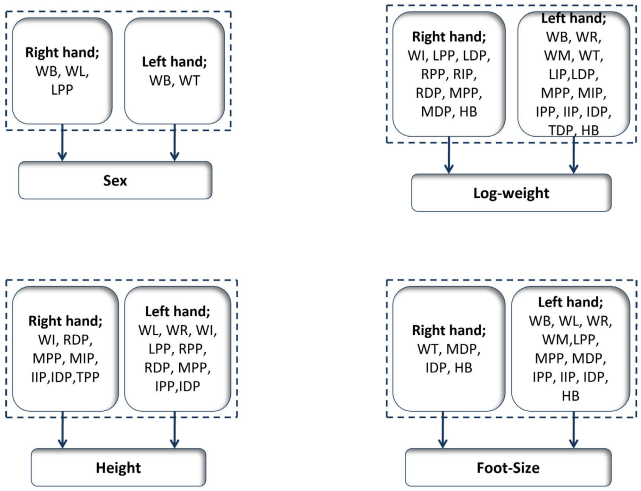

FIGURE 5. Model of extracted features.

(e) Nine (9) features for weight recognition from right hand as shown in Table 6.
(f) Thirteen (13) features for weight recognition from left hand as shown in Table 7.
(g) Four (4) features for foot-size recognition from right hand as shown in Table 8.
(h) Eleven (11) features for foot-size recognition from left hand as shown in Table 9.

To further visualize insight of selected features, we employed curve-fitting tool for generating fitting plot. Performance of fitting analysis is demonstrated using metric in Eq. (32). The results demonstrated that most of the selected features are statistically significant with R^2 of 0.2-1.0. It indicates that less significant features were below 0.65 which are still considered in our models development. Though these features are not proportionate for recognition task, can still serve as vital information for lessening complexity of designing hand camera rig and AI. Results show that not all features are equally significant in biometric gestures discrimination. This is required to validate whether ECOC-SVM and ANFIS-SC are sufficiently enough for recognizing demographic cues from biometric hand features.

D. RECOGNITION PHASE

We have selected SVM-ECOC and ANFIS-SC recognition algorithms to validate the selected biometric hand features. The two algorithms are constructed in MATLAB R2020a software. The selected parameter values for these algorithms

TABLE 6. Statistical confidence of selected features for Weight from right-hand.

Features	WI	LPP	LDP	RPP	RIP	RDP	MPP	MDP	HB	WEIGHT
WI	1									
LPP	0.3558	1								
LDP	0.61482	0.48575	1							
RPP	0.49913	0.75792	0.56994	1						
RIP	0.59371	0.37736	0.62123	0.47213	1					
RDP	0.52323	0.37063	0.68171	0.43944	0.36802	1				
MPP	0.37242	0.63139	0.6008	0.41953	0.52578	0.36836	1			
MDP	0.59019	0.39406	0.65245	0.45197	0.55532	0.64007	0.4941	1		
HB	0.66082	0.32041	0.51125	0.65234	0.48616	0.56761	0.59309	0.56934	1	
WEIGHT	0.15937	0.35854	0.47231	0.20798	0.41595	0.52046	0.043473	0.48309	0.61643	1

TABLE 7. Statistical confidence of selected features for Weight from left-hand.

Features	WB	WR	WM	WT	LIP	LDP	MPP	MIP	IPP	IIP	IDP	TDP	HB	WEIGHT
WB	1													
WR	0.67444	1												
WM	0.27781	0.9351	1											
WT	0.66728	0.63985	0.74453	1										
LIP	0.37361	0.51931	0.40719	0.39857	1									
LDP	0.65351	0.54203	0.59075	0.60681	0.34375	1								
MPP	0.54879	0.45239	0.43524	0.50677	0.43213	0.44387	1							
MIP	0.5339	0.54631	0.50845	0.48446	0.40065	0.51167	0.34688	1						
IPP	0.54586	0.48252	0.38931	0.40946	0.36538	0.52378	0.66891	0.66355	1					
IIP	0.54886	0.52996	0.59519	0.51499	0.62719	0.59863	0.45892	0.64177	0.19967	1				
IDP	0.55643	0.32047	0.38912	0.38744	0.51887	0.62148	0.27747	0.34226	0.51958	0.26709	1			
TDP	0.56825	0.49927	0.53647	0.35564	0.51494	0.40872	0.46174	0.56753	0.27292	0.57602	0.51858	1		
HB	0.5705	0.5904	0.75155	0.69213	0.45674	0.6413	0.59495	0.524	0.42099	0.47978	0.4767	0.5434	1	
WEIGHT	0.72429	0.48413	0.19556	0.53137	0.30875	0.54596	0.27204	0.49787	0.17023	o.44613	0.36195	0.49357	0.68883	1

TABLE 8. Statistical confidence of selected features for Foot-size from right-hand.

Features	WT	MDP	IDP	HB	FOOT-SIZE
WT	1				
MDP	0.56696	1			
IDP	0.56502	0.72574	1		
HB	0.62223	0.56405	0.53997	1	
FOOT-SIZE	0.74103	0.68382	0.6014	0.5844	1

are detailed in Table 10. The extracted features are shown in Fig. 5.

1) RECOGNITION USING SVM-ECOC

SVM is designed as explained in section II-B, to divide line between two classes and to maximize margin. To achieve multi-class binary recognition, we ensemble ECOC code with SVM. We have chosen kernel function in SVM algorithm for nonlinear intrinsic hand features evaluation, to enable more increase of features to fit hyper-plane. Biometric intrinsic hand features are divided into 70% training and 30% validation. The features are trained using SVM-ECOC algorithm for better optimization. $\gamma > 0$ is chosen (that is, $\gamma = 1/(2\sigma^2)$). Then, value of γ defines influence and extent to which training hand poses attain good accuracy. The values of γ and c are hyper-parameters tuned to attain optimum SVM-ECOC recognition. However, c find model tolerance towards misclassification, its low value yield low accuracy, while its high value yield good accuracy but may result to failure in generalization. We settled these hyper-parameters with middle values. Finally, we achieved SVM classifier with $w = \sum_{i=1}^{n} c_i O_i^s \phi(h_i)$, c_i which can be obtained through Error Correcting Output Code (ECOC) optimization problem solution. The ensemble ECOC code $\log_2 4 = 4$ is sufficient to characterize four different demographic classes. Extracted features are shown in Fig. 5 to represent multi-class labels $1, \cdots, 4$. However, if minimum Hamming distance among each pair of code words is E, then code may correct minimum $\frac{E(E-1)}{2}$ per bit errors. In as much as error Ψ distant away less than $\frac{E(E-1)}{2}$ from actual feature, the nearest feature is classified as correct one. This code can correct up to 2 errors per four input features, and can correct up to 3 errors per 13 biometric intrinsic hand features. As our number of classes E is $3 < E \leq 7$. Then per biometric intrinsic hand feature has length $2^{E-1} - 1$. Also, the matrix F needs 13 binary classifiers (i.e. 13 columns) altogether. Then finally, evaluation metrics are used to analyze performance of the SVM-ECOC algorithm.

2) RECOGNITION USING ANFIS-SC

ANFIS-SC is activated using randomly selected 70% and 30% of biometric intrinsic hand dataset for both training and validation phases, respectively. ANFIS-SC is adopted here to recognize size, height, weight and sex (O_i). The chosen parameter values of ANFIS-SC is described in Table 10. Accordingly, we achieved finest combination

TABLE 9. Statistical confidence of selected features for Foot-size from left-hand.

Features	WB	WL	WR	WM	LPP	MPP	MDP	IPP	IIP	IDP	HB	FOOT-SIZE
WB	1											
WL	0.52867	1										
WR	0.66695	0.95623	1									
WM	0.76225	0.87762	0.9408	1								
LPP	0.50375	0.29796	0.42504	0.76057	1							
MPP	0.48971	0.44989	0.49865	0.39775	0.40809	1						
MDP	0.23676	0.36257	0.37388	0.46935	0.35491	0.44726	1					
IPP	0.5159	0.47484	0.33115	0.59725	0.45779	0.63593	0.25013	1				
IIP	0.63266	0.48294	0.56798	0.57443	0.56758	0.35775	0.53156	0.28049	1			
IDP	0.44839	0.43257	0.25772	0.4135	0.28378	0.37248	0.53156	0.42473	0.29141	1		
HB	0.74806	0.38903	0.57125	0.69859	0.72803	0.56738	0.35479	0.39306	0.61324	0.46871	1	
FOOT-SIZE	0.81336	0.65876	0.53178	0.7649	0.80202	0.61133	0.37482	0.40295	0.51013	0.45512	0.79287	1

TABLE 10. Parameters choice of the proposed models.

Algorithm	Parameters	Values
ANFIS	Membership functions	14
	FIS generation algorithm	SC
	Max. Iteration	350
	No. of Inputs	21
	Initial step	0.01
	Decrease rate	0.009
	Increase rate	0.001
	Fuzzy rules	14
SVM	Kernel	RBF
	Box constraint	80
	Iteration	304
	K	5
	Solver	SMO
	Bias	29.599

of ANFIS model having maximum number of inputs h_i plus one output O^i, making 113 input-output vector, with fourteen (14) Gaussian MF in each biometric hand pose. Every feature takes in two parameters, generating one hundred and forty nonlinear parameters. The linear equations take in five parameters having fourteen (14) rules, which generate eighty four (84) linear parameters in total. The finest model is obtained with 0.3 as the value of cluster radius, versus three hundred and fifty maximum iteration. Furthermore, unlike SVM, ANFIS has complex non-linear projection. Thus it is suitable to learn biometric information.

E. PARAMETER SETTINGS

The following parameters in Table 10 are chosen for the two adopted AI algorithms design.

F. PERFORMANCE METRICS

The evaluation metrics are used to realized the performance of the input-feature models and the adopted algorithms, as given below. Variables O_i, O'_i, S,, θ, σ_r^2 and O_a denotes observed data, verified (predicted) features, number of samples, number of parameters, as well as mean observed features, respectively.

1) ROOT MEAN SQUARE ERROR (RMSE)

$$\mathbf{RMSE} = \sqrt{\frac{1}{S}\sum_{i=1}^{S}(O'_i - O_i)^2}. \tag{28}$$

2) MEAN ABSOLUTE PERCENTAGE ERROR (MAPE)

$$\mathbf{MAPE} = \frac{1}{S}\sqrt{\sum_{i=1}^{S}\left|\frac{O'_i - O_i}{O'_i}\right|}. \tag{29}$$

3) SCATTER INDEX (SI)

$$\mathbf{SI} = \sqrt{\frac{\sum_{i=1}^{S}[(O'_i - O'a) - (O_i - Oa)]^2}{\sum_{i=1}^{S}(O_i)^2}}. \tag{30}$$

4) MEAN ABSOLUTE DEVIATION (MAD)

$$\mathbf{MAD} = \frac{\sum_{i=1}^{S}(O_i - O_{a_i})}{S}. \tag{31}$$

5) COEFFICIENT OF DETERMINATION (R^2)

$$\mathbf{R}^2 = 1 - \frac{\sum_{i=1}^{S}(O_i - O'_i)^2}{\sum_{i=1}^{S}(O_i - O_{a_i})^2}. \tag{32}$$

Furthermore, we reported ANFIS-SC model's simplicity, flexibility and degree of fitness according to the following two metrics: Akaike's Information Criterion correction (AICc), and Nash-Sutcliffe model efficiency index (N-S).

6) AKAIKE'S INFORMATION CRITERION (AICC)

AIC estimate degree of information lost for a model [45]. If small number of datasets are employed for model development, AIC index may likely to overfit, thus corrected AIC (AICc) is formulated to handle AIC overfit. Small sample-size AICc metrics evaluate the quality of a model according to structural flexibility and level of deviation from average value. It is obtained during model's verification of unseen observations [25], [46]. Therefore, low value of AICc describes best model. AICc is computed as

$$\mathbf{A}ICc = \frac{(2\theta S + (Sln(\sigma_r^2)(S - \theta - 1))}{S - \theta - 1}. \tag{33}$$

TABLE 11. Generalization performance of AI algorithms for sex from right-hand features.

Approaches	AICc	MAD	MAPE	NSE	R^2	Adj R	RMSE	SI
SVM	39.55702	0.156409	0.107143	99.88042	0.5376	0.5334	0.365963	0.002701
LOG	45.07204	0.53901	0.307293	81.97302	0.5376	0.5334	0.343086	0.008494
M2 (WB+WL)	8.087221	0.166271	0.11912	99.66191	0.6865	0.6824	0.296887	0.008013
M3 (WB+LPP)	27.87367	0.247959	0.170029	99.54402	0.667113	0.662733	0.397156	0.009268
M4 (WL+LPP)	36.18139	0.356329	0.311969	99.37706	0.5324	0.5263	0.448766	0.009851
M1 Complete	**14.46776**	**0.170653**	**0.120847**	**99.92655**	**0.7930**	**0.7903**	**0.326093**	**0.008398**

TABLE 12. Generalization performance of AI algorithms for sex from left-hand features.

Approaches	AICc	MAD	MAPE	NSE	R^2	Adj R	RMSE	SI
SVM	39.55702	0.156409	0.09375	99.88042	0.5376	0.5334	0.365963	0.002701
ANFIS-SC	**25.08221**	**0.249754**	**0.173281**	**99.55869**	**0.6916**	**0.6876**	**0.381182**	**0.009079**

TABLE 13. Generalization performance of AI algorithms for height from right-hand features.

Approaches	AICc	MAD	MAPE	NSE	R^2	Adj R	RMSE	SI
SVM	736.2207	6.208281	0.036356	99.94597	0.3993	0.3999	8.206129	0.002701
LOG	779.11	7.480122	0.134923	77.2661	0.3593	0.3535	7.690868	0.11
M2 (WI+RDP)	235.9469	6.380283	0.037308	99.5862	0.66765	0.663277	8.469525	0.000443
M3 (WI+MIP)	236.0166	6.255062	0.036979	99.65877	0.679319	0.675099	8.478212	0.000444
M4 (RDP+MIP)	232.4787	6.524516	0.037811	99.42212	0.67397	0.66968	8.04838	0.000432
M5 (MIP+IIP)	243.4611	7.402342	0.044467	99.47995	0.541577	0.535545	9.459095	0.000469
M1 (complete)	**227.965**	**6.44006**	**0.036429**	**99.385**	**1**	**1**	**1.531497**	**0.000418**

TABLE 14. Generalization performance of AI algorithms for height from left-hand features.

Approaches	AICc	MAD	MAPE	NSE	R^2	Adj R	RMSE	SI
SVM	733.8027	5.899592	0.034006	99.94597	0.3557	0.3498	8.118025	0.000135
LOG	923.33	8.734011	0.047044	69.54017	0.3557	0.3498	7.712923	0.002861
M2 (WL+WR)	414.0269	6.396812	0.038063	99.56044	0.453084	0.445888	8.928602	0.000455
M3 (WR+WI)	232.122	5.99232	0.034637	99.53943	0.645707	0.641045	8.006275	0.000431
M4 (RPP+MPP)	244.3698	8.093233	0.046263	99.29911	0.426264	0.418715	9.586351	0.000472
M5 (RDP+MPP)	236.677	6.42746	0.037701	99.57538	0.599993	0.59473	8.560947	0.000446
M1 Complete	**2.39E+02**	**6.400739**	**0.037142**	**99.572**	**1**	**1**	**3.837685**	**0.000453**

7) NASH-SUTCLIFFE MODEL EFFICIENCY INDEX (NSE)

This metric is defined to evaluate the model fitness and the level of its deviation, it has an index value ranging from $-\infty$ to 1 [25]:

$$NSE = 1 - [\frac{\sum_{i=1}^{S}(O_i - O_i')^2}{\sum_{i=1}^{S}(O_i - O_i')^2}] \times 100. \quad (34)$$

IV. RESULTS AND ANALYSIS

In this section, performance results of two adopted algorithms according to generalization of demographic information are presented. Generalization performance of the algorithms is computed using well-defined evaluation metrics of section III-F. Our results demonstrated that optimized ANFIS model with SC tracks nonlinear data pattern of intrinsic hand features in most of the data pattern. ANFIS-SC outperforms optimized SVM with ECOC model. The best results were settled at model 1 (includes all the selected features from PCC scheme). Best results are illustrated bold-faced in Tables 11-18. The performance speed of the two algorithms are explained in section IV-B. However, optimized SVM-ECOC model outperforms conventional SVM from one of the existing model.

TABLE 15. Generalization performance of AI algorithms for weight from right-hand features.

Approaches	AICc	MAD	MAPE	NSE	R^2	Adj R	RMSE	SI
SVM	1311.627	7.010427	1.64032	99.45446	0.1610	0.1533	107.0889	0.001027
LOG	1421.045	7.949201	1.71392	7.176402	0.1610	0.1533	8.801442	0.003361
M2 (WI+HB)	251.6942	7.81854	0.113107	99.78958	0.540347	0.534299	10.67658	0.000836
M3 (LDP+RDP)	263.4964	9.779508	0.142146	99.64324	0.475929	0.469033	12.70016	0.000911
M4 (RPP+HB)	249.8986	7.373375	0.111724	99.76504	0.383308	0.375193	10.39834	0.000825
M5 (RDP+MDP)	260.7313	9.012506	0.130456	99.71084	0.368412	0.360101	12.19407	0.000893
M1 Complete	**250.8366**	**7.542391**	**0.114461**	**99.65008**	**1**	**1**	**0.14277**	**0.00083**

TABLE 16. Generalization performance of AI algorithms for weight from left-hand features.

Approaches	AICc	MAD	MAPE	NSE	R^2	Adj R	RMSE	SI
SVM	1311.566	6.313469	1.641854	99.3655	0.3258	0.3196	107.0599	0.001038
LOG	1433.172	9.895241	2.531001	6.993101	0.2610	0.3196	7.889831	0.003063
M2 (WR+WM)	262.8667	8.942322	0.143839	99.80356	0.676718	0.672464	12.58308	0.000907
M3 (WT+HB)	252.3266	7.80151	0.113307	99.77097	0.542257	0.536234	10.77633	0.00084
M4 (WM+HB)	258.0577	8.217767	0.119327	99.81876	0.610386	0.605259	11.72393	0.000876
M5 (WM+WT)	260.9679	9.191511	0.131805	99.73941	0.386448	0.378375	12.23657	0.000895
M1 Complete	**2.60E+02**	**9.410505**	**0.133198**	**99.71922**	**1.0000**	**1.0000**	**0.0000248**	**0.000887**

TABLE 17. Generalization performance of AI algorithms for foot-size from right-hand features.

Approaches	AICc	MAD	MAPE	NSE	R^2	Adj R	RMSE	SI
SVM	1408.337	6.781813	Infinity	99.27494	0.3506	0.3447	164.9105	0.010423
LOG	923.061	8.07492	0.043721	70.65912	0.3506	0.3447	7.743087	0.001202
M2 (MDP+IDP)	567.0301	1.435183	0.189593	99.60544	0.54345	0.537443	1.801605	0.001418
M3 (WT+HB)	524.1225	0.757061	0.114161	99.27277	0.746166	0.742826	0.958567	0.002215
M4 (WT+MDP)	109.8796	0.977643	0.143112	99.65819	0.629053	0.624173	1.326498	0.002606
M5 (WT+IDP)	110.3254	1.046634	0.152788	99.33081	0.681733	0.677545	1.335225	0.002614
M1 Complete	**-62.256**	**1.059786**	**0.148327**	**99.50138**	**0.918447**	**0.917374**	**1.140019**	**0.002619**

TABLE 18. Generalization performance of AI algorithms for foot-size from left-hand features.

Approaches	AICc	MAD	MAPE	NSE	R^2	Adj R	RMSE	SI
SVM	1408.716	6.867124	Inf	99.3251	0.2592	0.2524	165.1896	0.010432
LOG	1401.33	7.72093	0.40927	69.34901	0.2592	0.2524	8.27042	0.018201
M2 (WL+WR)	153.3784	1.673711	0.304124	99.82326	0.588992	0.583584	2.514895	0.003588
M3 (WR+WM)	129.4252	1.344965	0.200059	99.78837	0.657841	0.653339	1.76823	0.003008
M4 (WL+WM)	1.24E+02	1.308961	0.199876	99.54428	0.653163	0.648599	1.621235	0.002881
M5 (WB+WM)	107.7562	1.047615	0.149179	99.57157	0.740165	0.736746	1.285718	0.002565
M1 Complete	**122.8158**	**1.299598**	**0.181757**	**99.54061**	**1**	**1**	**0.604451**	**0.002866**

A. COMPARISON BETWEEN PERFORMANCE OF OPTIMIZED ANFIS-SC, SVM-ECOC AND SOME EXISTING MODELS

According to Table 19, our adopted algorithms are compared based on the work in [18]. Evaluation metrics in Section III-F were used, but in some metrics where conventional method did not utilize that terms, those places were left blank with dash to indicate that, metrics is not available. The comparison is made based on number of recognition accuracy, R^2, RMSE, AICc, MAD, and MAPE, respectively. The best result is achieved by ANFIS-SC. However, in some instances SVM-ECOC is computationally efficient compared to ANFIS-SC and LOG model. LOG models recognized majority features efficiently, while disregarding minority features as noise, which lead to mislcassification and low computed accuracy. In addition, comparison is made against performance of LOG-based classification as displayed in Table 20. Results indicate applicability and superior performance of ANFIS-SC in biometric recognition than the LOG-based method.

Moreover, ANFIS-SC model has superior performance when compared to other two models, therefore it is chosen

TABLE 19. Performance comparison between AI-based methods with state-of-the-art method.

Demographic features	Biometric features	Approaches		Evaluation Metrics					
				Accuracy	R^2	RSME	AICc	MAD	MAPE
SEX	Right Hand	Miguel-Hurtado et al. [19]	SVM	88.7	-	-	-	-	-
			LOG	81	-	-	-	-	-
		Our method	SVM-ECOC	90.89	0.5376	0.365963	39.55702	0.156409	0.107143
			LOG	89.37	0.5376	0.343086	45.07204	0.53901	0.307293
			ANFIS-SC	**94.87179**	**0.7930**	**0.326093**	**14.467756**	**0.170653092**	**0.120847**
	Left Hand	Miguel-Hurtado et al. [19]	SVM	78.3	-	-	-	-	-
			LOG	86	-	-	-	-	-
		Our method	SVM-ECOC	85.89	0.5376	0.365963	39.55702	0.156409	0.09375
			LOG	87.47	0.49952	0.398931	41.33946	0.34841	0.15296
			ANFIS-SC	**93.58974**	**0.6916**	**0.381182**	**25.082209**	**0.249754078**	**0.173281**

TABLE 20. Comparison of generalization performance between regression-based and AI-based recognition.

Demographic features	Biometric features	Approaches		Evaluation metrics				
				R^2	RSME	AICc	MAD	MAPE
Height	Right Hand	Miguel-Hurtado et al. [19]	LOG	0.56	6.4			
		Our method	**ANFIS-SC**	**1**	**1.531497**	**228**	**6.4**	**0.036429**
	Left Hand	Miguel-Hurtado et al. [19]	LOG	0.46	7.1			
		Our method	**ANFIS-SC**	**1**	**3.837685**	**2.39E+02**	**6.400739**	**0.037142**
Weight	Right Hand	Miguel-Hurtado et al. [19]	LOG	0.58	0.12			
		Our method	**ANFIS-SC**	**1**	**0.14277**	**250.8366**	**7.542391**	**0.114461**
	Left Hand	Miguel-Hurtado et al. [19]	LOG	0.66	0.11			
		Our method	ANFIS-SC	**1**	**0.0000248**	**-1538.5**	**0.000016**	**0.00000023**
Footsize	Right Hand	Miguel-Hurtado et al. [19]	LOG	0.78	1.12			
		Our method	**ANFIS-SC**	**0.918447**	**1.140019**	**-62.256**	**1.059786**	**0.148327**
	Left Hand	Miguel-Hurtado et al. [19]	LOG	0.73	1.26			
		Our method	**ANFIS-SC**	**1**	**0.604451**	**122.8158**	**1.299598**	**0.181757**

for further analysis according to two metrics: AICc index and NSE index. AICc is adopted due to our small sample size (S) and number of different parameters (θ). However, value of AICc is obtained from Equation (33), with 1.86. We observed that AICc from ANFIS-SC model achieved best result, which lead to good model flexibility. Smaller criterion of AICc depict model accuracy. In addition, final prediction error of ANFIS-SC Model is obtained as 2.815×10^{-6}. This value demonstrates that ANFIS-SC model has good generalization quality to biometric hand intrinsic cues. However, ANFIS-SC model fitness of 99% is achieved through evaluation of *NSE* metrics for the complete proposed features. Degree of model information lost is evaluated through AICc with good results and interpretation as detailed in Table 21. The value of η_{N-S} is obtained through Equation (34), with 98.99% model accuracy. Therefore, our obtained results demonstrates computational flexibility and soft computing of ANFIS-SC model to nonlinear datasets. Hence, this work focus only on the performance accuracy of the algorithms rather than speed performance of the adopted algorithms, however the following section present the algorithms' running time.

TABLE 21. Recognition error.

Demographic features	Biometric features	Accuracy	Error
SEX	RIGHT	94.87179	5.128205
	LEFT	93.58974	6.410256
HEIGHT	RIGHT	91.02564	8.974359
	LEFT	93.58974	6.410256
WEIGHT	RIGHT	93.58974	6.410256
	LEFT	94.87179	5.128205
FOOT-SIZE	RIGHT	89.74359	10.25641
	LEFT	90.39537	9.598633

B. RUNNING TIME

As described from Tables 22-23, running-time complexity for training and validating recognition of SVM-ECOC and ANFIS-SC algorithms are provided. Running-time complexities approximate all bounds of each algorithm during recognition of the selected biometric information. Running time from SVM-ECOC is obtained from its corresponding output, which comes from response of classifier f, parameter to observe whether recognition of SVM-ECOC classifiers can be averted to best recognition, and variable which select best input features to be used during validation φ. SVM-ECOC running time is given by:

$$T(R_u \aleph \varphi(n)^2). \tag{35}$$

TABLE 22. Computational time needed to model right hand features.

AI algorithm	Model	Time complexity	Time (sec.) Training	Testing
ANFIS-SC	Sex	$T(\aleph(n+n^2))$	2.09	0.33
	Height		15.12	1.59
	Weight		32.67	2.14
	Foot-size		12.81	1.66
SVM-ECOC	Sex	$T(\varphi+n\varphi)$	2.99	0.46
	Height		13.03	1.18
	Weight		45.54	4.92
	Foot-size		7.61	1.08

TABLE 23. Computational time needed to model Left Hand features.

AI algorithm	Model	Time complexity	Time (sec.) Training	Testing
ANFIS-SC	Sex	$T(\aleph(n+n^2))$	4.11	0.46
	Height		27.99	4.21
	Weight		48.52	6.79
	Foot-size		14.06	1.91
SVM-ECOC	Sex	$T(\varphi+n\varphi)$	5.49	0.99
	Height		12.88	1.72
	Weight		21.66	3.71
	Foot-size		55.06	7.81

However, training of SVM-ECOC algorithm may amount to run time from the following equation:

$$T(\aleph n\varphi) \times T(n) = T(\aleph\varphi(n)^2). \tag{36}$$

The running time during validation is given as $T(n)$. This is because the best models with good accuracy settle at n features, thus the overall run time complexity during validation can be formulated as follows:

$$T(n) + T(R_u\varphi n), \tag{37}$$

where T stand as big T (time complexity), R_u denote maximum number of upper bounds, $\aleph$ maximum number of iterations, n number of samples in the data set, φ number of selected features per each model combination. However, time taken to verify unseen inputs in SVM-ECOC algorithm raises based on the computation of $(\varphi \times n)$. This means that, it depend on the number of selected features and number of input sets. Therefore, it is finally settled at:

$$T(\varphi + n\varphi). \tag{38}$$

Furthermore, the ANFIS-SC run time can be obtained by computing the time complexity of SC and ANFIS. In what follows, the SC run time can be formulated as:

$$T(\aleph(n+n^2)). \tag{39}$$

SC time complexity, computed distance matrix among data set couplets, which need $T(nm^2)$ arithmetic operations. Since distance matrix is obtained, then, SC resulted in having equal number of iterations to that of the number of clusters. Per each cycle, the running time of Eq. (9) is given as $T(m)$. In general, ANFIS run time is observed from $T(1)$ which is the run time from fuzzy rules. Whereas, Eq. (2) has run time of $T(n)$ and Eq. (3) has run time $T(n^2)$. Thus, the total run time of ANFIS-SC is achieved by summing over all time complexity among the SC and ANFIS, as follows:

$$T(\aleph(nU + obj.U)) + T(1) + T(n) + T(n^2) = T(n^2), \tag{40}$$

where U and *obj.* denote number of solutions and objective function. Moreover, run time of the compared AI algorithms have brief implementation as compared to other methods.

Moreover, the major drawback of extending SC with ANFIS is the trial and error while selecting the most suitable and stable radius. This is due to a small cluster radius that may gives more centers, which as a result may lead to over-fitting. Whereas large cluster radius may lead to less centers, that may lead to under-fitting, as a result may decrease the recognition accuracy of the models.

V. CONCLUSION

In this work, we initialized AI algorithms using ECOC and subtractive clustering optimization schemes as potential enabler in conventional AIs to handle complex parameters estimation. The work aimed to investigates correlation among intrinsic hand measurements and demographic features. It particularly used AI algorithms and LOG for comparison to analyzed and recognize sex, height, weight, and foot-size from 21 hand features extracted through measurement of hand bones. The compared models are realized according to proper parameters chosen. The evaluation metrics show that AI recognition performed better than LOG while predicting demographic characteristics. Our results have shown to agree with and performed better than previous method. Specifically, ANFIS-SC based learning demonstrates high performance in terms of accuracy and speed, when compared to SVM-ECOC learning. ANFIS-SC learning results qualified it worthy in many applications such as crime detection and soft-biometric features recognition. This work has direct application in both biometric and forensic industries. The major limitations of both methods are related to accuracy and high number of computational burden for a limited number of the hand corpus. This means that, on restricted hand corpus, the quality of the biometric recognition of AI algorithms would be already rather good. Moreover, adding more demographic and psychological cues such as race/ethnicity, life expectancy, and facial marks can further improve the recognition capabilities by reducing the number of classification errors. In addition, AI algorithms yield premature and slow convergence.

ACKNOWLEDGMENT

The authors are also grateful to anonymous IEEE Access reviewers for their potential reviews and insightful comments. Chainarong Khunpanuk and Nuttapol Pakkaranang would like to thank Phetchabun Rajabhat University. Auwal Bala Abubakar would like to thank the Department of Mathematics and Applied Mathematics, Sefako Makgatho Health Sciences University.

REFERENCES

[1] M. Drahansky, M. Dolezel, J. Urbanek, E. Brezinova, and T.-H. Kim, "Influence of skin diseases on fingerprint recognition," *J. Biomed. Biotechnol.*, vol. 2012, pp. 1–14, May 2012.

[2] S. A. Haider, Y. Rehman, and S. M. U. Ali, "Enhanced multimodal biometric recognition based upon intrinsic hand biometrics," *Electronics*, vol. 9, no. 11, p. 1916, Nov. 2020.

[3] J. L. Blanch and S. S. Christensen, "Biometric basics: Options to gather data from digital devices locked by a biometric key," *Dept. Justice J. Federal Law Pract., United State Attorney's Bull.*, vol. 66, no. 2018, p. 3, Jan. 2018.

[4] T. Kanchan and P. Rastogi, "Sex determination from hand dimensions of north and south Indians," *J. Forensic Sci.*, vol. 54, no. 3, pp. 546–550, May 2009.

[5] R. Karki and P. Singh, "Gender determination from fingerprints," *J. Universal College Med. Sci.*, vol. 2, no. 1, pp. 12–15, May 2014.

[6] R. Guest, O. Miguel-Hurtado, S. V. Stevenage, G. J. Neil, and S. Black, "Biometrics within the SuperIdentity project: A new approach to spanning multiple identity domains," in *Proc. Int. Carnahan Conf. Secur. Technol. (ICCST)*, Oct. 2014, pp. 1–6.

[7] S.-C. Jee, S. Bahn, and M. H. Yun, "Determination of sex from various hand dimensions of Koreans," *Forensic Sci. Int.*, vol. 257, p. 521.e1, Dec. 2015.

[8] S.-C. Jee and M. H. Yun, "Estimation of stature from diversified hand anthropometric dimensions from Korean population," *J. Forensic Legal Med.*, vol. 35, pp. 9–14, Oct. 2015.

[9] M. K. Thakar, P. Kaur, and T. Sharma, "Validation studies on gender determination from fingerprints with special emphasis on ridge characteristics," *Egyptian J. Forensic Sci.*, vol. 8, no. 1, pp. 1–7, Dec. 2018.

[10] J. C. Loehlin, S. E. Medland, and N. G. Martin, "Relative finger lengths, sex differences, and psychological traits," *Arch. Sexual Behav.*, vol. 38, no. 2, pp. 298–305, Apr. 2009.

[11] A. K. Agnihotri, S. Agnihotri, N. Jeebun, and K. Googoolye, "Prediction of stature using hand dimensions," *J. Forensic Legal Med.*, vol. 15, no. 8, pp. 479–482, Nov. 2008.

[12] S. V. Stevenage, C. Walpole, G. J. Neil, and S. M. Black, "Testing the reliability of hands and ears as biometrics: The importance of viewpoint," *Psychol. Res.*, vol. 79, no. 6, pp. 989–999, Nov. 2015.

[13] O. Al-Jarrah and A. Halawani, "Recognition of gestures in Arabic sign language using neuro-fuzzy systems," *Artif. Intell.*, vol. 133, nos. 1–2, pp. 117–138, 2001.

[14] F. A. Mufarroha and F. Utaminingrum, "Hand gesture recognition using adaptive network based fuzzy inference system and K-nearest neighbor," *Int. J. Technol.*, vol. 8, no. 3, pp. 559–567, 2017.

[15] N. A. Alias and N. H. M. Radzi, "Fingerprint classification using support vector machine," in *Proc. 5th ICT Int. Student Project Conf. (ICT-ISPC)*, May 2016, pp. 105–108.

[16] M. L. Gavrilova, F. Ahmed, A. H. Bari, R. Liu, T. Liu, Y. Maret, B. K. Sieu, and T. Sudhakar, "Multi-modal motion-capture-based biometric systems for emergency response and patient rehabilitation," in *Research Anthology on Rehabilitation Practices and Therapy*. Hershey, PA, USA: IGI Global, 2021, pp. 653–678.

[17] W. K. Wong, F. H. Juwono, and B. T. T. Khoo, "Multi-features capacitive hand gesture recognition sensor: A machine learning approach," *IEEE Sensors J.*, vol. 21, no. 6, pp. 8441–8450, Mar. 2021.

[18] O. Miguel-Hurtado, R. Guest, S. V. Stevenage, G. J. Neil, and S. Black, "Comparing machine learning classifiers and linear/logistic regression to explore the relationship between hand dimensions and demographic characteristics," *PLoS ONE*, vol. 11, no. 11, Nov. 2016, Art. no. e0165521.

[19] S. Escalera, O. Pujol, and P. Radeva, "Separability of ternary codes for sparse designs of error-correcting output codes," *Pattern Recognit. Lett.*, vol. 30, no. 3, pp. 285–297, 2009.

[20] S. Escalera, O. Pujol, and P. Radeva, "On the decoding process in ternary error-correcting output codes," *IEEE Trans. Pattern Anal. Mach. Intell.*, vol. 32, no. 1, pp. 120–134, Jan. 2010.

[21] T. Windeatt and R. Ghaderi, "Coding and decoding strategies for multi-class learning problems," *Inf. Fusion*, vol. 4, no. 1, pp. 11–21, Mar. 2003.

[22] J. Benesty, J. Chen, Y. Huang, and I. Cohen, "Pearson correlation coefficient," in *Noise Reduction in Speech Processing*. Berlin, Germany: Springer, 2009, pp. 1–4.

[23] B. Kaur and G. Joshi, "Lower order Krawtchouk moment-based feature-set for hand gesture recognition," *Adv. Hum.-Comput. Interact.*, vol. 2016, pp. 1–10, Mar. 2016.

[24] S. Abdullahi and M. Gaya, "Forecasting of HOSR for different mobile carriers in Kano using conventional and intelligent techniques," *Int. J. New Comput. Archit. Appl.*, vol. 9, no. 1, pp. 1–11, 2019.

[25] S. B. Abdullahi, K. Muangchoo, A. B. Abubakar, A. H. Ibrahim, and K. O. Aremu, "Data-driven AI-based parameters tuning using grid partition algorithm for predicting climatic effect on epidemic diseases," *IEEE Access*, vol. 9, pp. 55388–55412, 2021.

[26] J. Zambrano, J. Sanchis, J. Herrero, and M. Martínez, "WH-EA: An evolutionary algorithm for Wiener–Hammerstein system identification," *Complexity*, vol. 2018, Feb. 2018, Art. no. 1753262.

[27] K.-K. Xu, H.-D. Yang, and C.-J. Zhu, "A novel extreme learning machine-based Hammerstein–Wiener model for complex nonlinear industrial processes," *Neurocomputing*, vol. 358, pp. 246–254, Sep. 2019.

[28] A. Wills and B. Ninness, "Generalised Hammerstein–Wiener system estimation and a benchmark application," *Control Eng. Pract.*, vol. 20, no. 11, pp. 1097–1108, Nov. 2012.

[29] E. Bai, "A blind approach to the Hammerstein–Wiener model identification," *Automatica*, vol. 38, no. 6, pp. 967–979, 2002.

[30] I. Ebtehaj and H. Bonakdari, "Design of a fuzzy differential evolution algorithm to predict non-deposition sediment transport," *Appl. Water Sci.*, vol. 7, no. 8, pp. 4287–4299, Dec. 2017.

[31] I. Ebtehaj, H. Bonakdari, and M. S. Es-haghi, "Design of a hybrid ANFIS–PSO model to estimate sediment transport in open channels," *Iranian J. Sci. Technol., Trans. Civil Eng.*, vol. 43, no. 4, pp. 851–857, Dec. 2019.

[32] A. Gholami, H. Bonakdari, I. Ebtehaj, B. Gharabaghi, S. R. Khodashenas, S. H. A. Talesh, and A. Jamali, "A methodological approach of predicting threshold channel bank profile by multi-objective evolutionary optimization of ANFIS," *Eng. Geol.*, vol. 239, pp. 298–309, May 2018.

[33] O. Kisi, "Streamflow forecasting and estimation using least square support vector regression and adaptive neuro-fuzzy embedded fuzzy c-means clustering," *Water Resour. Manage.*, vol. 29, no. 14, pp. 5109–5127, Nov. 2015.

[34] F. Moradi, H. Bonakdari, O. Kisi, I. Ebtehaj, J. Shiri, and B. Gharabaghi, "Abutment scour depth modeling using neuro-fuzzy-embedded techniques," *Mar. Georesources Geotechnol.*, vol. 37, no. 2, pp. 190–200, Feb. 2019.

[35] S. Mitaim and B. Kosko, "What is the best shape for a fuzzy set in function approximation?" in *Proc. IEEE 5th Int. Fuzzy Syst.*, vol. 2, Sep. 1996, pp. 1237–1243.

[36] D. A. Pisner and D. M. Schnyer, "Support vector machine," in *Machine Learning*. Amsterdam, The Netherlands: Elsevier, 2020, pp. 101–121.

[37] X. Tan, F. Yu, and X. Zhao, "Support vector machine algorithm for artificial intelligence optimization," *Cluster Comput.*, vol. 22, no. S6, pp. 15015–15021, Nov. 2019.

[38] N. Cristianini and J. Shawe-Taylor, *An Introduction to Support Vector Machines and Other Kernel-Based Learning Methods*. Cambridge, U.K.: Cambridge Univ. Press, 2000.

[39] T. G. Dietterich and G. Bakiri, "Solving multiclass learning problems via error-correcting output codes," *J. Artif. Intell. Res.*, vol. 2, pp. 263–286, Jan. 1995.

[40] O. Pujol, P. Radeva, and J. Vitria, "Discriminant ECOC: A heuristic method for application dependent design of error correcting output codes," *IEEE Trans. Pattern Anal. Mach. Intell.*, vol. 28, no. 6, pp. 1007–1012, Jun. 2006.

[41] O. Pujol, S. Escalera, and P. Radeva, "An incremental node embedding technique for error correcting output codes," *Pattern Recognit.*, vol. 41, no. 2, pp. 713–725, Feb. 2008.

[42] S. Escalera, O. Pujol, and P. Radeva, "Boosted landmarks of contextual descriptors and forest-ECOC: A novel framework to detect and classify objects in cluttered scenes," *Pattern Recognit. Lett.*, vol. 28, no. 13, pp. 1759–1768, Oct. 2007.

[43] A. A. Gonzalez, R. Bertschinger, and D. Saupe, "Modeling VO_2 and VCO_2 with Hammerstein–Wiener models," in *Proc. 4th Int. Congr. Sport Sci. Res. Technol. Support*, 2016, pp. 134–140.

[44] A. F. Morosini, S. S. Haghshenas, S. S. Haghshenas, and Z. W. Geem, "Development of a binary model for evaluating water distribution systems by a pressure driven analysis (PDA) approach," *Appl. Sci.*, vol. 10, no. 9, p. 3029, Apr. 2020.

[45] H. Akaike, "A new look at the statistical model identification," *IEEE Trans. Autom. Control*, vol. AC-19, no. 6, pp. 716–723, Dec. 1974.

[46] H. Bonakdari, H. Moeeni, I. Ebtehaj, M. Zeynoddin, A. Mahoammadian, and B. Gharabaghi, "New insights into soil temperature time series modeling: Linear or nonlinear?" *Theor. Appl. Climatol.*, vol. 135, nos. 3–4, pp. 1157–1177, 2019.

SUNUSI BALA ABDULLAHI (Member, IEEE) received the B.Sc. and M.Sc. degrees in electronics from Bayero University Kano (BUK), Nigeria. He is currently pursuing the Ph.D. degree with the King Mongkut's University of Technology Thonburi, Thailand. His current research interests include computer vision, artificial intelligence, nonlinear optimization and their applications in human motion analysis, data analysis, wireless systems, and social signal processing.

CHAINARONG KHUNPANUK received the bachelor's degree in mathematics from the Udonthani Teacher's College, in 1988, the master's degree in teaching mathematics from Chiang Mai University, and the Education Doctoral (Ed.D.) degree in mathematics education from the Curtin University of Technology, Australia. He is currently a Lecturer with the Mathematics and Computing Science Program, Faculty of Science and Technology, Phetchabun Rajabhat University. His research interests include equilibrium problem, iterative algorithms for solving nonlinear problems, number theory, and numerical analysis.

ZAKARIYYA ABDULLAHI BATURE received the B.Sc. (Hons.) and M.Sc. degrees in electronics from Bayero University Kano (BUK), Nigeria, in 2017 and 2019, respectively. He is currently pursuing the Ph.D. degree in electrical and information engineering technology with the King Mongkut's University of Technology Thonburi (KMUTT), Bangkok, Thailand. His research interests include computer vision, deep learning, eye tracking, and mobile communications.

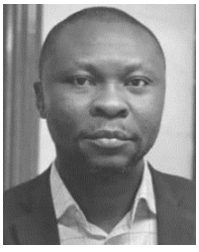

HARUNA CHIROMA received the B.Tech. degree in computer science and artificial intelligence from Abubakar Tafawa Balewa University, the M.Sc. degree in computer science and artificial intelligence from Bayero University Kano, and the Ph.D. degree in computer science and artificial intelligence from the University of Malaya. He is also a Teacher, interested specially in technology enhanced learning. He has been an external examiner for Ph.D. and M.Sc. students for universities. Presently, he is supervising 15 M.Sc. students and three Ph.D. students. He graduated seven M.Sc. and two Ph.D. students at Abubakar Tafawa Balewa University, Bauchi, Nigeria. His research interests include machine learning, neural networks with emphasis on deep learning, nature inspired algorithms and their applications in the Internet of Vehicles, self-driving vehicles, big data analytics, emerging cloud computing architecture, natural language processing, computer vision, and the IoT. He has published over 120 academic articles relevant to his research interest in different venues, including ISI WoS or Scopus indexed journals, such as but not limited to *Artificial Intelligence Review* (Springer), *Neural Networks World*, *Neural Computing and Applications* (Springer), *Journal of Ambient Intelligence and Humanized Computing* (Springer), *Supercomputing* (Springer), *Applied Soft Computing* (Elsevier), and *Intelligent Automation and Soft Computing* (Taylor & Francis). He is an Associate Editor of IEEE Access, Q1, Impact Factor 4.09, (ISI WoS or Scopus Indexed). He is also an Associate Editor of *Telecommunication Computing Electronics and Control journal* (TELKOMNIKA, Scopus Indexed), an Editorial Board Member of *Recent Advances in Computer Science and Communications* (Scopus Indexed), and a Guest Editor of *Mathematical Problems in Engineering* (ISI or Scopus indexed) and *BioMed Research International* (ISI or Scopus indexed). He is an Editor of three edited books published by Springer Berlin Heidelberg. He is an Invited Reviewer for over 30 ISI WoS indexed journals, such as *Applied Soft Computing* (Elsevier), *Artificial Intelligence Review* (Springer), *Knowledge-Based System* (Elsevier), *International Journal of Bio-Inspired Computation* (Inderscience), and *Neural Computing and Applications* (Springer). He has served in different capacities in more than 30 international conferences, workshops, and symposiums. He was invited by QS world universities ranking, in 2017, 2018, and 2019, to evaluate research strength of universities in computer science.

NUTTAPOL PAKKARANANG received the bachelor's degree (Hons.) in mathematics from Maejo University, in 2014, and the master's and Ph.D. degrees in applied mathematics from the King Mongkut's University of Technology Thonburi. He is currently a Lecturer with the Mathematics and Computing Science Program, Faculty of Science and Technology, Phetchabun Rajabhat University. Now, he has more than 55 publications published in *Science* journal. His research interests include convex optimization problems with application in signal and image processing, nonlinear problems in geodesic spaces, and numerical analysis.

AUWAL BALA ABUBAKAR received the master's degree in mathematics and the Ph.D. degree in applied mathematics from the King Mongkut's University of Technology Thonburi, Thailand, in 2015. He is currently a Lecturer with the Department of Mathematical Sciences, Faculty of Physical Sciences, Bayero University Kano, Nigeria. He is the author of more than 70 research articles. His main research interests include methods for solving nonlinear monotone equations with application in signal recovery and image restoration.

ABDULKARIM HASSAN IBRAHIM was born in Sokoto, Nigeria. He received the B.Sc. degree in mathematics from Usmanu Danfodiyo University Sokoto, Nigeria, and the Ph.D. degree in applied mathematics from the King Mongkut's University of Technology Thonburi, Bangkok, Thailand. He has authored and coauthored several research articles indexed in either Scopus or Web of Science. His current research interests include numerical optimization and image processing. In August 2018, he was awarded the Petchra Pra Jom Klao Scholarship to study the Ph.D. degree.